Iron Twin-Coronet Porphyrins as Models of Myoglobin and Hemoglobin: Amphibious Electrostatic Effects of Overhanging Hydroxyl Groups for Successful CO/O_2 Discrimination**

Fumito Tani,*[a] Mikiya Matsu-ura,[a] Kiyoko Ariyama,[a] Toshikazu Setoyama,[a] Takayuki Shimada,[b] Shinjiro Kobayashi,[a] Takashi Hayashi,[c] Takashi Matsuo,[c] Yoshio Hisaeda,[c] and Yoshinori Naruta*[a]

Abstract: Inspired by the observation of polar interactions between CO and O_2 ligands and the peptide residues at the active site of hemoglobin and myoglobin, we synthesized two kinds of superstructured porphyrins: **TCP-IM**, which contains a linked imidazole ligand, and **TCP-PY**, which contains a linked pyridine ligand, and examined the thermodynamic, kinetic, and spectroscopic (UV/Vis, IR, NMR, and resonance Raman) properties of their CO and O_2 complexes. On both sides of each porphyrin plane, bulky binaphthyl bridges form hydrophobic cavities that are suitable for the binding of small molecules. In the proximal site, an imidazole or pyridine residue is covalently fixed and coordinates axially to the central iron atom. In the distal site, two naphtholic hydroxyl groups overhang toward the center above the heme. The CO affinities of **TCP**s are significantly lower than those of other heme models. In contrast, **TCP**s have moderate O_2 binding ability. Compared with reported model hemes, the binding selectivity of O_2 over CO in **TCP-IM** and **TCP-PY** complexes is greatly improved. The high O_2 selectivity of the **TCP**s is mainly attributable to a low CO affinity. The comparison of k_{on}(CO) values of **TCP**s with those of unhindered hemes indicates the absence of steric hindrance to the intrinsically linear CO coordination to Fe^{II} in **TCP-IM** and **TCP-PY**. The abnormally large k_{off}(CO) values are responsible for the low CO affinities. In contrast, $k_{off}(O_2)$ of **TCP-PY** is smaller than those of other pyridine-coordinated model hemes. For the CO adducts of **TCP**s, unusually low ν(Fe–CO) and unusually high ν(C–O) frequencies are observed. These results can be ascribed to decreased back-bonding from the iron atom to the bound CO. The lone pairs of the oxygen atoms of the hydroxyl groups prevent back-bonding by exertion of a strong negative electrostatic interaction. On the other hand, high $\nu(Fe-O_2)$ frequencies are observed for the O_2 adducts of **TCP**s. In the resonance Raman (RR) spectrum of oxy-**TCP-IM**, we observed simultaneous enhancement of the $Fe-O_2$ and O–O stretching modes. Furthermore, direct evidence for hydrogen bonding between the hydroxyl groups and bound dioxygen was obtained by RR and IR spectroscopy. These spectroscopic data strongly suggest that O_2 and CO binding to **TCP**s is controlled mainly by the two different electrostatic effects exerted by the overhanging OH groups: destabilization of CO binding by decreasing back-bonding and stabilization of O_2 binding by hydrogen bonding.

Keywords: dioxygen ligands · electrostatic interactions · heme proteins · hydrogen bonds · porphyrinoids

[a] Dr. F. Tani, Prof. Dr. Y. Naruta, M. Matsu-ura, K. Ariyama, T. Setoyama, Dr. S. Kobayashi
Institute for Fundamental Research of Organic Chemistry
Kyushu University, Higashi-ku, Fukuoka 812-8581 (Japan)
Fax: (+81) 92-642-2715
E-mail: naruta@ms.ifoc.kyushu-u.ac.jp

[b] T. Shimada
Department of Biological and Environmental Chemistry
Kyushu School of Engineering, Kinki University
Iizuka, Fukuoka 820-8555 (Japan)

[c] Dr. T. Hayashi,[+] Dr. T. Matsuo,[+] Prof. Dr. Y. Hisaeda
Department of Chemistry and Biochemistry
Graduate School of Engineering, Kyushu University
Higashi-ku, Fukuoka 812-8581 (Japan)

[+] Member of PRESTO in Japan Science and Technology Corporation

[**] Abbreviations used in this text: 1-MeIm = 1-methylimidazole; 1,2-Me_2Im = 1,2-dimethylimidazole; Py = pyridine; Pip = piperidine; $FePiv_3$5CIm = *meso*-5α,10α,15α-tris(*o*-pivalamidophenyl)-20β-{*o*-[5-(*N*-imidazolyl)valeramido]phenyl}porphyrinatoiron; FePocPiv = 5,10,15-((1,3,5-benzenetriyltriacetyl)tris(α,α,α-*o*-aminophenyl))-20-(α-*o*-pivalamidophenyl)porphyrinatoiron; Fe(PF3CUIm) = *meso*-5α,10α,15α-tris(*o*-pivalamidophenyl)-20β-{*o*-{[3-(*N*-imidazolyl)propyl]ureido}phenyl}porphyrinatoiron; Fe(PF3CUPy) = *meso*-5α,10α,15α-tris(*o*-pivalamidophenyl)-20β-{*o*-{[3-(3-pyridyl)-propyl]ureido}phenyl}porphyrinatoiron; Fe-aBHP(C_9Im)-(C_{12}) = α-5,15-[2,2′-(dodecanediamido)diphenyl]:β-10,20-[2,2′-(5-imidazol-1-ylnonane-1,9-diamido)diphenyl]porphyrinatoiron; Fe-aBHP($C_3 \cdot Py \cdot C_3$)-(C_{12}) = α-5,15-[2,2′-(dodecamethyleneamido)diphenyl]:β-(10,20)-{2,2′-[3,3′-(pyridine-3,5-diyl)dipropioamido]diphenyl}porphyrinatoiron; Fe-eBHP-($C_3 \cdot Py \cdot C_3$)(C_{12}) = α-5,15-[2,2′-(dodecamethyleneoxy)diphenyl]:β-(10,20)-{2,2′-[3,3′-(pyridine-3,5-diyl)dipropoxy]diphenyl}porphyrinatoiron; Fe(TpivPP) = 5,10,15,20-tetrakis[*o*-(pivalamido)phenyl]porphyrinatoiron; Fe(C_2Cap) = 5,10,15,20-{pyromellitoyltetrakis[*o*-(oxyethoxy)phenyl]}porphyrinatoiron; FeTTPPP = 5,10,15,20-tetrakis(2,4,6-triphenylphenyl)porphyrinatoiron; Fe(Piv_2C_{10}) = α,α-5,15-[2,2′-(decanediamido)diphenyl]-α,α-10,20-bis(*o*-pivalamidophenyl)porphyrinatoiron; Fe(TPP) = 5,10,15,20-tetraphenylporphyrinatoiron; Fe(OEP) = octaethylporphyrinatoiron; Fe(Piv_2C_8) = α,α-5,15-[2,2′-(octanediamido)diphenyl]-α,α-10,20-bis(*o*-pivalamidophenyl)porphyrinatoiron; Co(α^4-T_{neo}PP) = tetrakis[α^4-*o*-(neopentylcarboxamido)phenyl]porphyrinatocobalt(II)

0947-6539/03/0904-0862 $ 20.00+.50/0 *Chem. Eur. J.* **2003**, *9*, No. 4

Introduction

For several decades, researchers have investigated the mechanism of CO and O_2 discrimination in myoglobin (Mb) and hemoglobin (Hb).[1] The CO affinities of simple hemes are much higher than for O_2, by a factor of roughly 20000, but this ratio is reduced to 25–200 in Mb and Hb. This dramatic difference allows Mb and Hb to function effectively in O_2 storage and transport in the presence of the endogenous poison CO, which is produced during the breakdown of heme by heme oxygenase.[2] It had long been assumed that CO/O_2 discrimination is based mainly on distal steric constraints.[3] However, the results of structural, spectroscopic, mutagenic, and theoretical studies have highlighted the importance of polar interactions in the binding pocket.[4] The most significant distal effect invoked in the stabilization of O_2 in Mb and Hb is hydrogen bonding between coordinated O_2 and the distal histidine residue, which was initially proposed by Pauling.[5] This hydrogen bond was clearly identified by neutron diffraction studies on the oxy-myoglobin complex[4a] and by spectroscopic studies on cobalt-substituted myoglobins and hemoglobins.[6] Several groups reported that replacement, by site-directed mutagenesis, of the distal histidine residue in the binding pocket by hydrophobic groups produces major changes in the affinity and dissociation rate for O_2, but minor ones for CO.[1a] An extreme example of a hydrogen-bonded O_2 complex was observed for a unique Hb from the bloodworm *Ascaris*.[7] This Hb has a tyrosine instead of a histidine residue as hydrogen-bonding donor and has a remarkably high O_2 affinity, nearly 10^4 times that of mammalian Hb. The origin of this high O_2 affinity is believed to be 1) a strong hydrogen bond between tyrosine (Tyr-B10) and the terminal oxygen atom, 2) a weak hydrogen bond between glutamine (Gln-E7) and the proximal oxygen atom, and 3) a hydrogen bond between the above two amino acid residues.[8] The importance of hydrogen bonding for the stabilization of an oxy complex was also shown for some model compounds.[9]

Synthetic models of Hb and Mb have been invaluable in unraveling the subtle complexities of reversible O_2 binding and competitive inhibition by CO.[10] The earliest structurally and functionally elegant iron porphyrin model of the Hb and Mb active sites was the "picket-fence" porphyrin reported by Collman et al.[11] This porphyrin binds dioxygen reversibly at room temperature with a high affinity, similar to those of Hb and Mb. However, the CO affinity was 2–3 orders of magnitue higher than those of Hb and Mb. With the aim of controlling the CO affinity, other models including capped,[12] cyclophane,[13] pocket,[14] hybrid,[9a] and bis-handle porphyrins[15] were synthesized. Systematically decreasing the size of the available distal cavity decreased CO affinity, while leaving O_2 affinity roughly comparable to those of unmodified porphyrins. Such distal steric hindrance can significantly affect ligand binding, and this effect is manifested primarily in diminished ligand-association rate constants.

Because the question of steric inhibition of CO binding has been proposed in the context of the globins, the preparation of a new chemical model, which can regulate CO affinity by a nonsteric mechanism, was highly desirable. However, in contrast to the steric control of CO binding, there have been no reports of models for investigating electrostatic suppression of CO binding except for our **SCP** (single-coronet porphyrin)[16a] and **TCP**s (twin-coronet porphyrins),[16b] presumably because of the synthetic challenges. To realize CO/O_2 discrimination by polar effects at a binding site without steric hindrance, a model must fulfill two requirements: 1) reduce CO affinity by polar interactions, and 2) form a stable O_2 adduct. We already gave a preliminary report on CO/O_2 discrimination by electrostatic effects exerted by overhanging hydroxyl groups in **SCP**.[16a] However, direct spectroscopic evidence for these effects were not fully obtained, because the dioxygen adduct of **SCP** was thermally unstable. We then synthesized second-generation models of superstructured porphyrins (**TCP-IM**, and **TCP-PY**, Scheme 1). On both sides of the porphyrin plane, bulky binaphthyl groups form hydrophobic molecular cavities, which are suitable for the binding of small molecules. In the proximal site, the imidazole (**TCP-IM**) and pyridine (**TCP-PY**) ligands are covalently fixed to coordinate axially to the central iron(II) center and are sterically well sheltered. Porphyrin **TCP-IM** is expected to be a more accurate model of Mb and Hb than **TCP-PY**, because of the axial imidazole ligand. In the distal site, two naphtholic hydroxyl groups are oriented toward the center above the heme. Based on the spectroscopic data of **TCP-PY**–CO complex, we already reported that the strong negative polar effect arising from the vicinal hydroxyl groups in the cavity prevent π back-bonding from the Fe^{II} dπ to the CO π* orbital.[16b] The decreased back-bonding leads to the exceptionally low CO affinity of **TCP-PY**. Here we describe studies on the CO and O_2 complexes of **TCP-IM** and **TCP-PY** by thermodynamic, kinetic, and spectroscopic methods. Compared to other models, the binding selectivity of O_2 over CO in **TCP-IM** and **TCP-PY** is greatly improved. This comprehensive study on **TCP**–CO and –O_2 complexes definitely established that CO/O_2 discrimination is realized mainly by the two different polar effects exerted by the overhanging hydroxyl groups: 1) destabilization of the CO complex by supressing π back-bonding from the iron atom to bound CO, and 2) stabilization of O_2 complex by hydrogen bonding to bound O_2.

Results and Discussion

Synthesis: **TCP**[17] was employed as the common framework of **TCP-IM** and **TCP-PY**. The latter was synthesized and characterized as described previously.[16b] As shown in Scheme 1, the synthetic route for the preparation of **TCP-IM**, which contains an axial imidazole ligand, is analogous to that for the preparation of **TCP-PY**. The imidazole moiety is attached to one of the inner hydroxyl groups of **1**. The chemical shifts of the imidazole protons in **2** are significantly shifted to higher field due to the porphyrin ring current (Im-CH: $\delta = 4.59$, 2.37 pp; Im-NCH_3: $\delta = -1.43$ ppm). Insertion of iron into the free-base porphyrin **2** (M = H_2) proceeds smoothly in high yield, in spite of the expected steric hindrance around the hydroxyl groups. The resultant iron(III) species **TCP-IM**-Cl was characterized by various spectroscopic methods. The ESR spectrum of **TCP-IM**-Cl exhibits

  0947-6539/03/0904-0863 $ 20.00+.50/0

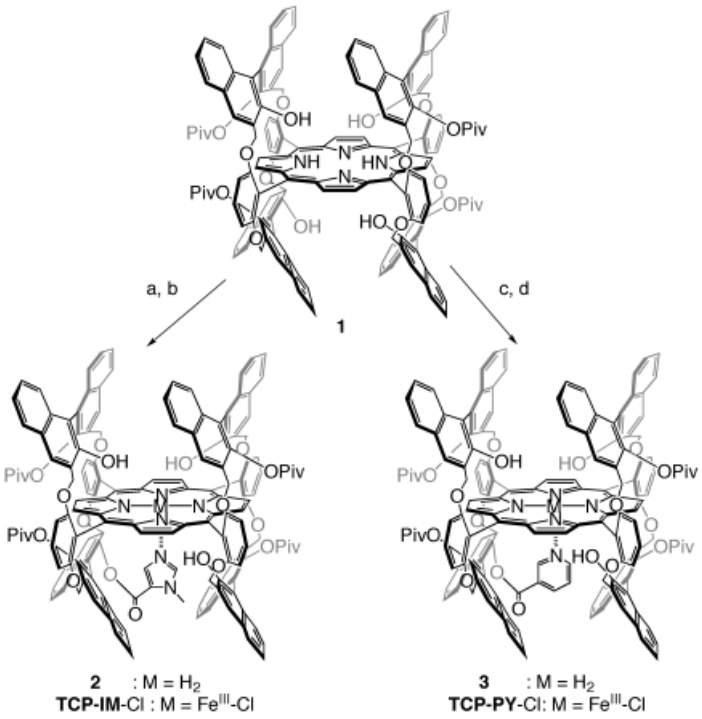

Scheme 1. a) 1-Methyl-5-imidazolecarboxylic acid, 1-(3-dimethylaminopropyl)-3-ethylcarbodiimide hydrochloride (EDC), CH_2Cl_2, 45%. b) [Fe(CO)$_5$], I_2, toluene, 50°C, 66%. c) Nicotinic acid, EDC, 4-dimethylaminopyridine, CH_2Cl_2, 57%. d) [Fe(CO)$_5$], I_2, toluene, 50°C, 70%.

typical high-spin signals ($g = 5.94$, 2.04). Iron(II) deoxy-**TCP-IM** and deoxy-**TCP-PY** were obtained by dithionite reduction of the corresponding iron(III) complexes.

CO and O_2 binding affinity: The electronic absorption spectra of the deoxy, CO, and O_2 complexes of **TCP-IM** are shown in Figure 1, and their λ_{max} values are summarized in Table 1 along with those of **TCP-PY**. The half-life times $\tau_{1/2}$ of the O_2 adducts are several days in toluene at 25°C. The irreversible oxidation of these O_2 adducts is effectively supressed by the bulky binaphthalene groups and the hydroxyl groups at the binding site. Due to the stability of the O_2 and CO adducts of **TCP-IM** and **TCM-PY**, the O_2 and CO binding affinity could be directly determined by photometric titration.[18, 19] Clear

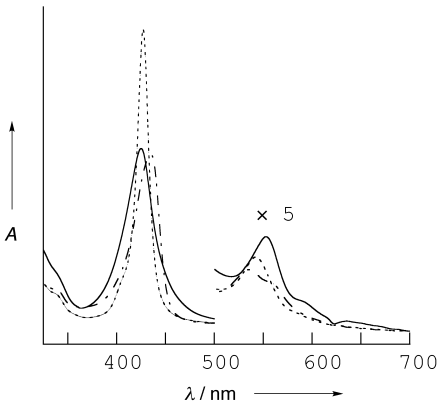

Figure 1. UV/Vis spectra of O_2, CO, and deoxy complexes of **TCP-IM** in toluene at 25°C: ——, O_2 adduct; - - - -, CO adduct; –•–, deoxy complex.

Table 1. Electronic absorption data for deoxy, CO and O_2 complexes of **TCP**s.[a]

Complex	λ_{max} [nm]
[Fe^{II}(**TCP-IM**)]	435, 535
[Fe(CO)(**TCP-IM**)]	427, 542
[Fe(O_2)(**TCP-IM**)]	425, 553
[Fe^{II}(**TCP-PY**)]	431, 534
[Fe(CO)(**TCP-PY**)]	428, 541
[Fe(O_2)(**TCP-PY**)]	424, 551

[a] In toluene, RT.

isosbestic points are observed in all UV/Vis spectra on increasing the O_2 or CO partial pressure in toluene (Figure 2). The binding affinities of the **TCP**s are summarized in Table 2 and are compared with those for hemoproteins and other heme models. Some models have intramolecularly linked imidazole or pyridine ligands and no significant steric strain in the distal site, except for FePocPiv(1-MeIm), which has an external axial ligand and steric hindrance in the binding site.

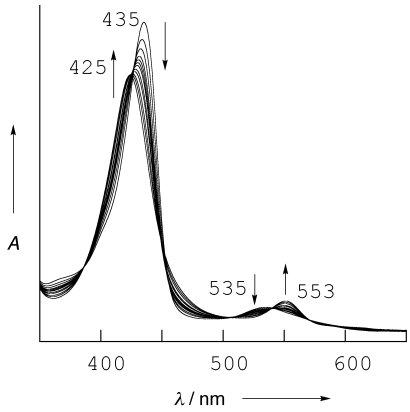

Figure 2. UV/Vis spectral change upon O_2 binding to **TCP-IM**. [**TCP-IM**] = 10 μM in toluene, 25.0°C.

The CO affinities of **TCP-IM** and **TCP-PY** are significantly lower than those of other heme models that have no steric strain in the binding site and are comparable to those of Hb and Mb. The CO affinity of **TCP-IM** is similar to that of the sterically hindered pocket porphyrin. The decrease of the CO affinities in **TCP**s has been rationally explained by the strong, negative electrostatic interaction with bound CO.[16b] On the other hand, **TCP**s have moderate O_2 binding ability, and the O_2 affinity of **TCP-IM** is comparable to that of Mb. It is considered that the hydrogen bonding to bound O_2 contributes to these reasonable O_2 affinities (vide infra). The influence of hydrogen bonding on O_2 affinity has been shown in both natural and model systems. For example, Momenteau et al. revealed that replacing the ether linkages in basket-handle porphyrins with amide linkages causes an approximately tenfold increase in O_2 affinity, while the affinity for CO is almost unaffected.[25] Site-directed mutagenesis of the distal histidine residue of Mb to glycine led to a tenfold decrease in O_2 affinity.[1a]

Compared to the conventional model hemes, the selectivities for oxygen relative to carbon monoxide [$M = P_{1/2}(O_2)/P_{1/2}$(CO)] in **TCP-IM** and **TCP-PY** complexes are substantially

0947-6539/03/0904-0864 $ 20.00+.50/0 *Chem. Eur. J.* **2003**, *9*, No. 4

Table 2. Kinetic and equilibrium parameters for CO and O_2 binding in hemoproteins and model hemes.

	k_{on}(CO) [$M^{-1}s^{-1}$]	k_{off}(CO) [s^{-1}]	$P_{1/2}$(CO) [Torr]	k_{on}(O_2) [$M^{-1}s^{-1}$]	k_{off}(O_2) [s^{-1}]	$P_{1/2}$(O_2) [Torr]	M	Ref.
Mb	$3-5\times10^5$	$1.5-40\times10^{-3}$	$1.4-2.5\times10^{-2}$	$1-2\times10^7$	10–30	0.37–1	20–40	[20]
Hb, R state	4.6×10^6	9×10^{-3}	1.4×10^{-3}	3.3×10^7	13.1	0.22	150	[21]
chelated protoheme	1.1×10^7	2.5×10^{-2}	2.3×10^{-4}	6.2×10^7	4200	5.6	24000	[20, 22]
chelated mesoheme	1.1×10^7	ca. 5×10^{-2}	5.6×10^{-4}	9.0×10^7	5000	4.9	10000	[23]
$FePiv_3$5CIm	3.6×10^7	7.8×10^{-3}	2.2×10^{-5}	4.3×10^8	2900	0.58	26600	[18a]
FePocPiv(1-MeIm)	5.8×10^5	8.6×10^{-3}	1.5×10^{-3}	2.2×10^6	9	0.36	270	[18a]
Fe(PF3CUIm)	2.9×10^7	1.4×10^{-2}	4.9×10^{-5}	2.6×10^8	3900	1.26	26000	[24]
Fe(PF3CUPy)	4.8×10^7	0.33	6.4×10^{-4}	3.0×10^8	190000	52.2	76000	[24]
Fe-aBHP(C_9Im)(C_{12})	4×10^7	6.7×10^{-3}	1.7×10^{-5}	3.1×10^8	620	0.29	17000	[25]
Fe-aBHP($C_3\cdot$Py$\cdot C_3$)(C_{12})	3.5×10^7	3×10^{-2}	9×10^{-5}	3.6×10^8	5000	2	22000	[25]
Fe-eBHP($C_3\cdot$Py$\cdot C_3$)(C_{12})	6.8×10^7	6.9×10^{-2}	1×10^{-4}	3×10^8	40000	18	180000	[25]
TCP-IM	2.1×10^7	0.23	1.1×10^{-3}	4.0×10^7	2000	1.3	1180	this work
TCP-PY	1.6×10^7	3.2	1.7×10^{-2}	2.7×10^7	2500	9.4	550	this work

improved (**TCP-IM**: 1180, **TCP-PY**: 550) as a result of the major contributions from the unusually low CO affinities.[26]

In the picket-fence system, changing the axial ligand from imidazole to pyridine leads to an approximately 40-fold decrease in O_2 affinity and a 13-fold decrease in CO affinity.[24] As a result, the O_2 selectivity decreases on replacement of imidazole with pyridine. A similar tendency is also observed for the basket-handle porphyrins.[25] However, in the case of our models, **TCP-PY** is superior to **TCP-IM** in O_2 binding selectivity. This reversal is attributed mainly to the O_2 affinity of **TCP-IM**, whose value is lower than that predicted from the O_2 affinity of **TCP-PY**. These results are discussed further below in the context of the kinetic data.

The thermodynamic parameters for dioxygen binding are summarized in Table 3.[32] The parameters of **TCP-IM** and **TCP-PY** are nearly identical: ΔH and ΔS (25 °C, 1 atm, in toluene) are -12.8 kcal mol^{-1}, -30 e.u. (**TCP-IM**) and -12.2 kcal mol^{-1}, -32 e.u. (**TCP-PY**), respectively. Model **TCP-IM** is slightly favored in both enthalpy and entropy terms. These parameters of **TCP-IM** and **TCP-PY** are comparable to those of mammalian Hb.[20b, 28] However, due to the complexity of cooperative O_2 binding by Hb, meaningful comparisons of ΔH and ΔS for the oxygenation process cannot be made.

Table 3. Thermodynamic parameters for O_2 binding to hemoproteins and model hemes.

Complex	$P_{1/2}$(O_2) [Torr]	ΔH [kcal mol^{-1}]	ΔS [e.u.]	Ref.
Mb, mammalian	0.5–1.3	-19 to -13.2	-50 to -38	[20b, 27]
Hb, mammalian	ca. 10	-10 to -15	-26 to -33	[20b, 28]
$FePiv_3$5CIm	0.58	-16.3	-40	[29]
FeTPivPP(1,2-Me_2Im)	38	-14.3	-42	[29]
Fe(C_2Cap)(1-MeIm)	23	-10.5	-28	[30]
Fe(C_2Cap)(1,2-Me_2Im)	4000	-9.7	-36	[30]
Fe(C_2Cap)(py)	180	-11.8	-37	[30]
FeTTPPP(1,2-Me_2Im)	508	-14.4	-47	[31]
TCP-IM	1.3	-12.8	-30	this work
TCP-PY	9.4	-12.2	-32	this work

Kinetics of CO and O_2 binding: The binding dynamics of CO and O_2 were explored by laser flash photolysis.[18, 33] Solutions of **TCP-IM**–CO or **TCP-PY**–CO in toluene exhibit good linear decay plots of $\log\Delta A$ versus t (Figure 3). The values of k_{on}(CO), calculated by Equation (1), did not change as the concentration of CO in solution was increased from 75 to 1500 μM. The k_{off}(CO) values were calculated from K(CO) and k_{on}(CO) by using Equation (2). The flash photolysis of stable O_2 adducts was also carried out over a range of O_2 concentrations (182–1820 μM). The values of k_{on}(O_2) and k_{off}(O_2) were determined by using Equation (3). The kinetic parameters for the binding of CO and O_2 to **TCP-IM** and **TCP-PY** are summarized in Table 2.

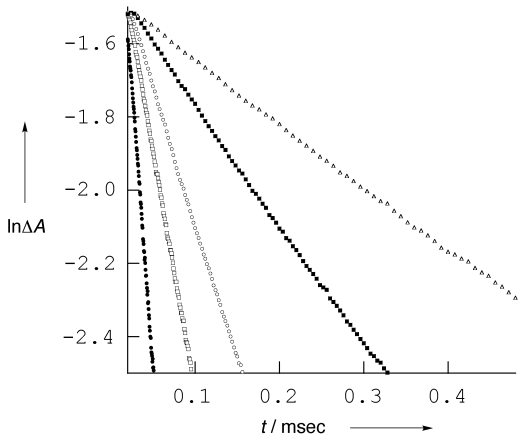

Figure 3. Determination of k_{on}(CO) of **TCP-PY**, obtained by flash photolysis of **TCP-PY**-CO in the presence of 75–1500 μM CO. [**TCP-PY**] = 10 μM in toluene, 25.0 °C, λ = 428 nm. [CO] = 1500 mM (●), 750 mM (□), 375 mM (○), 150 mM (■), 75 mM (△).

$$k_{obs} = k_{on}(L)[L] \quad (1)$$

$$K(L) = k_{on}(L)/k_{off}(L) \quad (2)$$

$$k_{obs} = k_{on}(L)[L] + k_{off}(L) \quad (3)$$

The k_{on}(CO) values of **TCP-IM** and **TCP-PY** are similar to those for model hemes without distal steric hindrance. Therefore, we concluded that there is probably no steric hindrance to incoming CO in **TCP-IM** and **TCP-PY**. Nevertheless, the k_{off}(CO) values of **TCP-IM** and **TCP-PY** are extremely large, that is, the destabilization of the CO

complexes results in the extremely low CO affinity, which originates from the negative electrostatic effect in the distal site of **TCP**s (vide infra). Contrary to our results, kinetic studies on sterically hindered pocket porphyrin[18a] indicate that distal steric hindrance significantly diminishes the rate constant for ligand association. For the O_2 adducts, the values of $k_{on}(O_2)$ are slightly lower compared to other models. The $k_{off}(O_2)$ value of **TCP-PY** – O_2 is smaller than those of other pyridine-coordinated heme models. This decrease is caused by the hydrogen bonding between bound oxygen and the phenolic hydroxyl groups in the molecular cavity, an effect revealed by RR and IR spectroscopy (vide infra). When the axial ligand is changed from pyridine to imidazole, the higher π basicity of imidazole (Im) relative to pyridine (Py) results in a large decrease in the k_{off} values (picket-fence porphyrins: 190000 (Py) → 2900 (Im);[24] basket-handle porphyrins: 5000 (Py) → 620 (Im).[25] However, in the present case, only a slight reduction (2500 → 2000) was observed. Traylor et al. reported that the k_{off} values of the O_2 adducts increase greatly on introducing distortions into the coordination sites of chelated hemes, and this leads to reduced O_2 binding affinities.[34] In our models, a larger distortion in the axial-base coordination in **TCP-IM** than in **TCP-PY** may result in the increase in the O_2 dissociation rate for **TCP-IM**.[35] To elucidate the mechanism of this effective CO/O_2 discrimination in **TCP**s, we next examined the CO and O_2 adducts by various spectroscopic methods.

Spectroscopic characterization of the CO adducts: The vibrational frequencies and ^{13}C chemical shifts of the CO complexes of **TCP**s and other hemes are summarized in Table 4. The spectroscopic features observed for **TCP-IM** – CO are very similar to those of **TCP-PY** – CO.[16b] CO isotopic substitution clearly reveals a sensitive band at 470 cm^{-1} in the RR spectrum of **TCP-IM** – ^{12}CO, which shifts to 467 cm^{-1} upon exchange with ^{13}CO. The IR spectrum of **TCP-IM** – CO exhibits a ν(C–O) band at 1994 cm^{-1}. The observed frequencies of **TCP-IM** – CO are unusually lower in ν(Fe–CO) and higher in ν(C–O) than the reported frequencies for hemoproteins and other chemical models. In the ^{13}C NMR spectrum, significant shielding of the ^{13}C signal is also observed in **TCP-IM** – CO.[42] Therefore, it is concluded that the unusual vibrational frequencies and the chemical shifts of **TCP** – CO complexes are due to the negative polar effect in the binding site.[16b] The hydroxyl groups in the distal site of **TCP**s play the decisive role: the decrease in back-donation is caused by the strong negative electrostatic interactions of bound CO with the lone pairs of the hydroxyl groups in the molecular cavity (Scheme 2). We conclude that the decrease in backdonation leads to the decreased CO affinities in **TCP**s.

Table 4. Vibrational frequencies and ^{13}C chemical shifts of CO adducts in hemoproteins and model hemes.

	ν(Fe–CO) [cm^{-1}] ^{12}CO (^{13}CO)	ν (C–O) [cm^{-1}] ^{12}CO (^{13}CO)	$\delta(^{13}C)$	Ref.
sperm whale Mb	507 (504)	1947	207.9	[36]
human Hb, α chain	507 (503)	1951 (1908)	206.4	[37]
FeTPivP(1-MeIm)	489 (485)	1969	204.7	[3a, 38]
Fe(PocPiv)(1-MeIm)	500 (496)	1964	204.6	[38c, 39]
Fe(Piv_2C_{10})(1-MeIm)	497 (494)	1952 (1910)	205.3	[38c, 40]
Fe(C_2-Cap)(1-MeIm)	497 (493)	2002 (1958)	202.1	[38c, 41]
TCP-IM	470 (467)	1994 (1948)	201.6	this work
TCP-PY	465 (460)	2008 (1964)	202.3	[16b]

Spectroscopic characterization of the O_2 adducts: Figure 4 displays the low-frequency region of the RR spectra of **TCP-IM** – O_2 and **TCP-PY** – O_2 in toluene at room temperature. The specific bands observed at 586 and 583 cm^{-1} in these spectra are shifted down field by 26 and 25 cm^{-1}, respectively, on $^{18}O_2$ isotope substitution. Therefore, we assign these bands as ν(Fe–O_2) modes. These shifts are close to those induced by

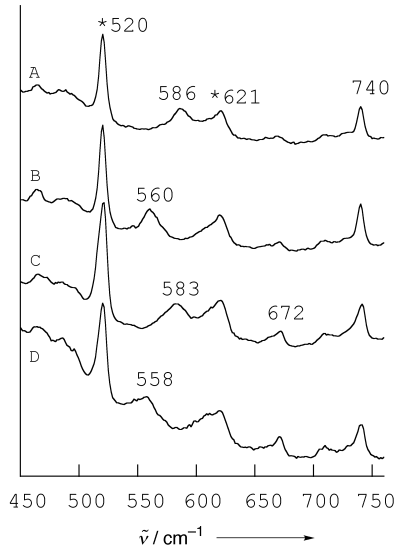

Figure 4. Low-frequency region of RR spectra of O_2 adducts of **TCP-IM** and **TCP-PY**. Toluene, room temperature, 413.1 nm excitation, and 20 mW: trace **A**, **TCP-IM**-$^{16}O_2$; trace **B**, **TCP-IM**-$^{18}O_2$; trace **C**, **TCP-PY**-$^{16}O_2$; trace **D**, **TCP-IM**-$^{18}O_2$. Asterisks indicate solvent peaks.

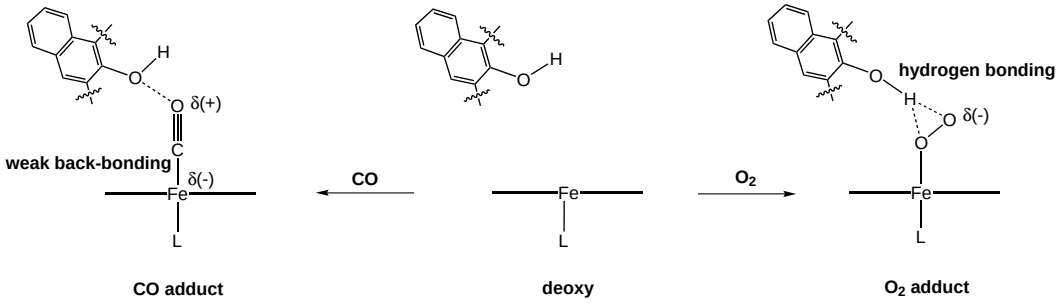

Scheme 2. Back-bonding and hydrogen bonding in CO and O_2 adducts.

0947-6539/03/0904-0866 $ 20.00+.50/0 *Chem. Eur. J.* **2003**, *9*, No. 4

the same isotopic substitution in oxy hemoproteins. It is noteworthy that the $\nu(Fe-O_2)$ frequencies for the O_2 complexes of **TCP-IM** and **TCP-PY** are significantly higher than those of hemoproteins and other heme models (Table 5). The higher $\nu(Fe-O_2)$ frequencies are considered to arise from the superstructures of **TCP**s; the inner hydroxyl groups are expected to form hydrogen bonds to the bound O_2.

Table 5. $\nu(Fe-O_2)$ frequencies for O_2 adducts of hemoproteins and model hemes.

	$\nu(Fe-O_2)/cm^{-1}$ $^{16}O_2$ ($^{18}O_2$)	Conditions	Ref.
sperm whale Mb	573 (549)	pH 8.2	[52]
Hb A	572(544)	pH 8.5, 10 °C	[53]
Fe(TpivPP)(1-MeIm)	571	CH_2Cl_2	[54]
Fe(OEP)(1-MeIm)	572	CH_2Cl_2, −120 °C	[55]
Fe{$(Piv)_2$-C_8}(1-MeIm)	563 (539)	toluene, 25 °C	[40]
TCP-IM	586 (560)	toluene, RT	this work
TCP-IM	599 (570)	toluene, −40 °C	this work
TCP-PY	583 (558)	toluene, RT	this work
TCP-PY	590 (563)	toluene, −40 °C	this work

In the high-frequency region of the RR spectra of **TCP**–O_2 complexes, ν_4 and ν_2, which are known to be sensitive to variations in the oxidation and spin state of the iron atom,[43] are observed at 1369, 1565 cm^{-1} (**TCP-IM**) and 1368, 1564 cm^{-1} (**TCP-PY**), respectively. The ν_4 bands are upshifted by 5 cm^{-1} upon conversion from CO to O_2 complexes of **TCP-IM** and **TCP-PY**.[44] This shift of the ν_4 band is attributed to the stronger π acidity of O_2 relative to CO.

In the region from 1000 to 1200 cm^{-1} (Figure 5), weak O_2-sensitive bands were observed at 1105 and 1132 cm^{-1}, which shifted to around 1050 cm^{-1} upon $^{18}O_2$ substitution. Moreover, a slight increase in intensity of the band at 1068 cm^{-1} was

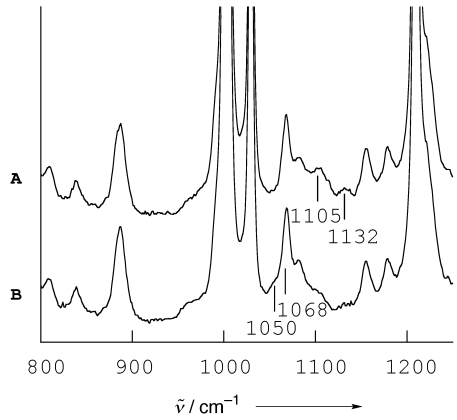

Figure 5. High-frequency region of RR spectra of O_2 adducts of **TCP-IM**. Toluene, room temperature, 413.1 nm excitation, 20 mW: trace **A**, **TCP-IM**-$^{16}O_2$; trace **B**, **TCP-IM**-$^{18}O_2$.

observed in the $^{18}O_2$ spectrum. Although unambiguous assignment is difficult due to the low intensity and overlap with another porphyrin bands, we consider these bands (1132, 1105, 1068, 1050 cm^{-1}) as candidates for $\nu(O-O)$ modes.[45] There is no definite consensus on the assignment of the O–O stretching mode in oxy hemoproteins, because the band displays substantial vibrational coupling with the internal modes.[46] Indeed, the observed isotopic shifts in **TCP-IM**–O_2 are not in perfect agreement with the value calculated from the harmonic oscillator approximation of the O–O stretching vibration. The vibrational coupling is also expected in the present case. Moreover, the ν(O–O) mode has not been reported in the resonance Raman spectra of globins and their models in which an iron-containing heme is coordinated by an axial N ligand.[47] The O–O stretching frequency has been measured by RR spectroscopy after replacing the iron atom of the heme with cobalt.[6, 48] Very recently, Rousseau et al. reported direct Raman spectroscopic observation of both the $Fe-O_2$ and O–O stretching modes in hemoglobins from *Chamydomonas eugametos* and *Synechocystis* PCC6803.[49] These hemoproteins contain a tyrosine residue at helical position B10 and a glutamine residue at E7 instead of the histidine residue in the distal heme pocket. They suggested that distal-specific polar interactions could contribute to the enhancement of $\nu(O-O)$ by altering the energy levels of the molecular orbitals of the $Fe-O_2$ moiety. We also considered that the RR enhancement of the $\nu(O-O)$ mode could be ascribed to the polar effect of the hydroxyl groups in **TCP-IM**. Our chemical model is the first in which the $Fe-O_2$ and O–O stretching modes were simultaneously observed by RR spectroscopy. It is notable that $\nu(O-O)$ frequency of **TCP-IM** is considerably lower than that of other heme models (Fe(TpivPP)(1-MeIm)O_2: 1159 cm^{-1};[3a] Fe(TPP)(Pip)O_2: 1157 cm^{-1}[50]). We have also reported that the RR spectrum of oxy-**CoSCP** with **AdIm**(**2-H**) showed an unusually low $\nu(O-O)$ frequency. These low-frequency shifts were attributed to the cooperative effect of strong donation from **AdIm**(**2-H**) and hydrogen bonding between the inner hydroxyl groups and coordinated dioxygen.[51]

To confirm the expected hydrogen bonding, we performed the RR measurements on oxy-**TCP**s at low temperatures. Figure 6 compares the RR spectra of **TCP**–O_2 complexs at −45 °C and room temperature. When solutions of the oxygen adducts of the **TCP**s are cooled to −45 °C, the $\nu(Fe-O_2)$ frequencies of oxy-**TCP-IM** and **TCP-PY** are shifted to 599 and 590 cm^{-1}, respectively.[56] Shifts of similar magnitude are observed for the corresponding $^{18}O_2$ adducts on cooling from room temperature (**TCP-IM**: 560, **TCP-PY**: 558 cm^{-1}) to −45 °C (**TCP-IM**: 570, **TCP-PY**: 563 cm^{-1}). No other bands exhibited shifts on cooling. In terms of the experimental accuracy, the observed shifts are meaningful values. These results can be interpreted as an indication that the relatively weak $O-H\cdots O_2$ hydrogen bond at room temperature could be strengthened at −45 °C owing to decreased thermal motion of **TCP**s. Nakamoto et al. reported the $\nu(O-O)$ frequency shift of [Co(α^4-T_{neo}PP)(1-MeIm)O_2] in a variable-temperature experiment.[57] The $\nu(O-O)$ band appeared at 1142 cm^{-1} at room temperature and was shifted to 1137 cm^{-1} at about −90 °C. Our results and those of Nakamoto et al. suggest that strengthening the hydrogen bond enhances back-bonding from the metal atom to the bound dioxygen, which in turn increases the $\nu(M-O_2)$ frequency and decreases the $\nu(O-O)$ frequency.

We further examined the IR bands of the naphtholic hydroxyl groups of the **TCP**s. The IR spectra of deoxy-,

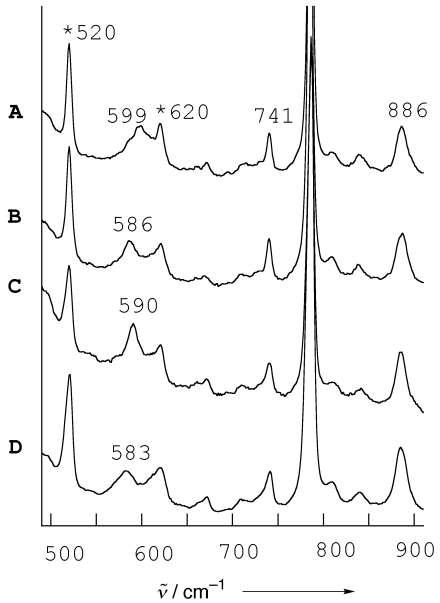

Figure 6. Temperature-dependent RR spectra of O_2 adducts of **TCP-IM** and **TCP-PY**. Toluene, 413.1 nm excitation, 20 mW: trace **A**, **TCP-IM**-$^{16}O_2$, $-45\,^{\circ}C$; trace **B**, **TCP-IM**-$^{16}O_2$, room temperature; trace **C**, **TCP-PY**-$^{16}O_2$, $-45\,^{\circ}C$; trace **D**, **TCP-IM**-$^{16}O_2$, room temperature. Asterisks indicate solvent peaks.

carbonyl-, and oxy-**TCP-IM** are illustrated in Figure 7. The deoxy and CO forms exhibit relatively strong ν(O–H) bands at 3464 cm^{-1}. The O_2 adduct has a lower frequency ν(O–H) band which is lower in intensity than the corresponding bands observed for the deoxy and CO forms. These results provide strong support that the bound dioxygen in **TCP**s interacts with the adjacent hydroxyl groups and forms hydrogen bonds (Scheme 2).[58]

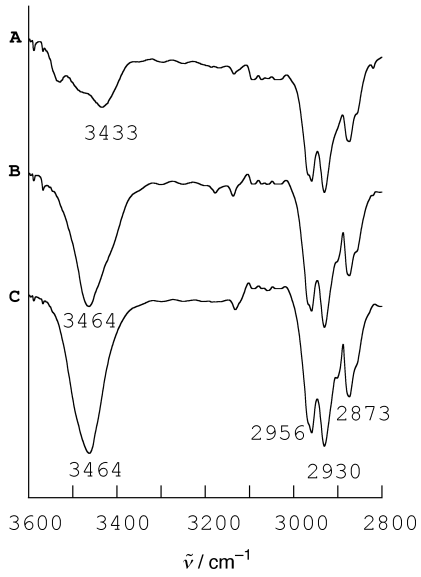

Figure 7. IR spectra of deoxy, CO, and O_2 complexes of **TCP-IM** in the OH region at room temperature. Difference spectra of deoxy, CO, and O_2 minus benzene: trace **A**, **TCP-IM**-O_2; trace **B**, **TCP-IM**-CO; trace **C**, **TCP-IM**-deoxy.

Conclusion

To unravel the subtle complexities of CO/O_2 binding in hemoproteins, sophisticated models, which have hydroxyl groups in the distal site without causing any steric hindrance and a covalently fixed axial ligand, were synthesized. The stable CO and O_2 adducts of **TCP-IM** and **TCP-PY** were obtained at room temperature: the half-lives $\tau_{1/2}$ of the O_2 adducts are several days in toluene at 25 °C. The CO affinities of **TCP**s are lower than those of sterically unhindered heme models, and comparable to those of Mb and Hb. These significantly lower CO affinities are considered to be due to the weak back-bonding in the CO adducts. The spectroscopic features of **TCP**–CO complexes, for example, the unusually low ν(Fe–CO) and high ν(C–O) frequencies, clearly indicate supression of back-bonding by the strong negative polar effect of the hydroxyl groups in the molecular cavity. The O_2 affinities of **TCP** are reasonably high, and the O_2 affinity of **TCP-IM** is comparable to those of Hb and Mb. As a result, the affinities for O_2 relative to CO in **TCP-IM** and **TCP-PY** complexes are high in spite of the absence of steric hindrance. We conclude that hydrogen bonding to bound O_2 is a major reason for the the O_2 affinity and the stability of the O_2 complexes. Direct evidence for hydrogen bonding, such as unusually high and temperature-dependent ν(Fe–O_2) frequencies, was obtained by vibrational spectroscopy. In addition, the RR spectrum of oxy-**TCP-IM** showed simultaneous enhancement of the Fe–O_2 and O–O stretching modes. This is the first observation of these bands in chemical heme models. The polar effect of the vicinal hydroxyl groups is considered to contribute to enhancement of the ν(O–O) mode in the RR spectra. The hydroxyl groups act as proton donors in the hydrogen-bonding interaction in the O_2 complexes. It is remarkable that the hydroxyl groups can provide both electronically negative and positive environments, that is, amphibious electrostatic effects, towards bound small molecules. The present results could highlight the importance of the polar interactions in heme chemistry and could shed light on the mechanism of CO/O_2 discrimination.

Experimental Section

All experimental details are as in reference [16b].

Synthesis of 2: Compound **1** (51 mg, 0.02 mmol) and 1-methyl-5-imidazolecarboxylic acid (126 mg, 1.00 mmol) were separately dried in vacuo for 2–3 h and then introduced into a glove box. They were mixed with 1-(3-dimethylaminopropyl)-3-ethylcarbodiimide hydrochloride (191 mg, 1.00 mmol). The reaction flask was cooled to 0 °C under N_2, and dry CH_2Cl_2 (9 mL) was added. After stirring overnight at room temperature, the formation of **2** was checked by TLC. The reaction mixture was quenched with water and then extracted with CH_2Cl_2. The combined organic layers were washed successively with saturated aqueous $NaHCO_3$, water, and brine, and then dried over Na_2SO_4. After removal of the solvent, the crude product was purified by flash column chromatography (silica gel, CH_2Cl_2/EtOH). Compound **2** was obtained as a purple solid (24 mg, 9.84×10^{-3} mmol, 45 %). ^{1}H NMR (400 MHz, $CDCl_3$): $\delta = 8.85$ (dd, $J = 4.4$, 4.6 Hz, 2H; pyrrole β-H), 8.69 (d, $J = 4.6$ Hz, 1H; pyrrole β-H), 8.63 (dd, $J = 4.6$, 4.4 Hz, 2H; pyrrole β-H), 8.49 (d, $J = 4.6$ Hz, 1H; pyrrole β-H), 8.20 (d, $J = 4.6$ Hz, 1H; pyrrole β-H), 8.16 (d, $J = 4.9$ Hz, 1H; pyrrole β-H), 8.05 (s, 1H), 7.96 (d, $J = 8.1$ Hz, 1H), 7.91 (s, 1H), 7.88 (s, 1H), 7.83–6.61 (m, 40H), 6.54 (m, 1H), 6.40 (m, 2H), 6.09 (t, 2H), 5.95–5.84 (m, 2H), 5.37 (d,

0947-6539/03/0904-0868 $ 20.00+.50/0 *Chem. Eur. J.* **2003**, *9*, No. 4

$J = 9.3$ Hz, 1H), 5.26–5.14 (m, 8H), 4.84–4.77 (m, 6H), 4.69 (d, $J =$ 14.1 Hz, 1H; benzyl CH_2), 4.59 (s, 1H; imidazole CH), 4.30 (d, $J =$ 13.7 Hz, 1H; benzyl CH_2), 4.14 (d, $J = 13.4$ Hz, 1H; benzyl CH_2), 2.69 (d, $J = 13.7$ Hz, 1H; benzyl CH_2), 2.56 (d, $J = 13.7$ Hz, 1H; benzyl CH_2), 2.37 (s, 1H; imidazole CH), 0.78 (s, 9H; piv CH_3), 0.68 (s, 9H; piv CH_3), 0.30 (s, 9H; piv CH_3), 0.22 (s, 9H; piv CH_3), −1.43 (s, 1H; imidazole NCH_3), −3.24 ppm (s, 2H; NH); UV/Vis (toluene): λ_{max} ($10^{-3}\varepsilon$) = 326 (30.8), 339 (28.9), 421 (304), 518 (18.0), 585 (6.01), 638 nm ($1.70\,M^{-1}cm^{-1}$); IR (neat): $\tilde{\nu} = 3450$, 3328, 3312, 3062, 2964, 2931, 2876, 1746, 1585, 1455, 1367, 1260, 1231, 1110, 1081, 795, 749, 718 cm^{-1}; HR-MS (FAB^+): *m/z* calcd for $C_{157}H_{124}N_6O_{21}$: 2428.8820; found: 2428.8813.

TCP-IM-Cl: Compound **2** (20.2 mg, 8.31×10^{-3} mmol) was dissolved in dry toluene (17 mL) and heated at 50 °C under N_2. [$Fe(CO)_5$] (371 μL, 2.82 mmol) and a solution of I_2 in toluene (23.9 mg, 94.2×10^{-3} mmol) were added. The mixture was stirred overnight in the dark, quenched with water, and then extracted with CH_2Cl_2. After removal of the solvent and drying, the residue was purified by flash column chromatography (silica gel, CH_2Cl_2/EtOH). The eluent was washed with brine, dried over NaCl, and freed from solvent to give **TCP-IM**-Cl (13.6 mg, 5.48×10^{-3} mmol, 66 %). UV/Vis (toluene): λ_{max} ($10^{-3}\varepsilon$) = 327 (31.7), 340 (32.9), 426 (83.7), 514 (9.07), 581 (2.86), 654 nm ($2.17\,M^{-1}cm^{-1}$); IR (neat): $\tilde{\nu} = 3450$, 3055, 2970, 2933, 2874, 1747, 1586, 1456, 1368, 1276, 1258, 1233, 1110, 1081, 996, 787, 749, 720 cm^{-1}; ESR (toluene, 4 K): $g = 5.94$, 2.04; HR-MS (FAB^+): *m/z* calcd for $C_{157}H_{121}O_{21}N_6Fe$: 2481.7934; found: 2481.7949; elemental analysis calcd (%) for $C_{157}H_{121}N_6O_{21}FeCl \cdot 4H_2O$: C 72.78, H 5.02, N 3.24; found: C 72.88, H 4.88, N 3.41.

Kinetic measurements: Laser flash photolysis was carried out by using a Nd-YAG laser (532 nm Continuum Powerlite 9010). The laser flash modules used were a pulsed 150 W xenon arc source (Applied Photophysics), a grating monochrometor (Chromex 250m), and a photomultiplier for 185–850 nm (Hamamatsu C6700). The concentration of the metalloporphyrin was 10 μM in toluene, and the temperature was regulated at 25.0 ± 0.1 °C with a circulator (Tokyo Rikakikai NCB-3200). The gaseous ligands were always present in large excess relative to the heme so that a pseudo-first-order approximation could be applied.

Acknowledgement

This research was financially supported by Grant-in-Aids for COE Research (no. 08CE2005 to Y.N.) and for Scientific Research on Priority Areas (no. 11228207 to Y.N.) from the Ministry of Education, Culture, Sports, and Technology, Japan, Grant-in-Aid for Scientific Research (A) (no. 14204073 to Y.N.) from Japan Society for the Promotion of Science (JSPS), and by Research Grants to F.T. from Takeda Science Foundation and Otsuka Chemical Co. M.M. gratefully acknowledges the JSPS Research Fellowships for Young Scientists. Kyushu University Projects in Research "Green Chemistry" partially supported this research.

[1] a) B. A. Springer, S. G. Sligar, J. S. Olson, G. N. Phillips, Jr., *Chem. Rev.* **1994**, *94*, 699; b) G. B. Jameson, J. A. Ibers in *Bioinorganic Chemistry* (Eds.: I. Bertini, H. B. Gray, S. J. Lippard, J. S. Valentine), University Science Books, Mill Valley, CA, **1994**, pp. 167, and references cited therein; c) F. Draghi, A. E. Miele, C. Travaglini-Allocatelli, B. Vallone, M. Brunori, Q. H. Gibson, J. S. Olson, *J. Biol. Chem.* **2002**, *277*, 7509.

[2] T. Sjostrand, *Acta Physiol. Scand.* **1952**, *26*, 334.

[3] a) J. P. Collman, J. I. Brauman, T. R. Halbert, K. S. Suslick, *Proc. Natl. Acad. Sci. USA* **1976**, *73*, 3333; b) L. Stryer in *Biochemistry*, 3rd ed., Freeman, New York, **1988**, p. 149.

[4] a) S. E. V. Phillips, B. P. Schoenborn, *Nature* **1981**, *292*, 81; b) B. Shaanan, *Nature* **1982**, *296*, 683; c) T. G. Spiro, P. M. Kozlowski, *J. Biol. Inorg. Chem.* **1997**, *2*, 516; d) J. S. Olson, G. N. Phillips, Jr., *J. Biol. Inorg. Chem.* **1997**, *2*, 544; e) T. G. Spiro, P. M. Kozlowski, *Acc. Chem. Res.* **2001**, *34*, 137; f) M. L. Quillin, R. M. Arduini, J. S. Olson, G. N. Phillips, Jr., *J. Mol. Biol.* **1993**, *234*, 140; g) G. S. Kachalova, A. N. Popov, H. D. Bartunik, *Science* **1999**, *284*, 473; h) K. Chu, J. Vojtchovsky, B. H. McMahon, R. M. Sweet, J. Berendzen, I. Schlichting, *Nature* **2000**, *403*, 921.

[5] L. Pauling, *Nature* **1964**, *203*, 182.

[6] T. Kitagawa, M. R. Ondrias, D. L. Rousseau, M. Ikeda-Saito, T. Yonetani, *Nature* **1982**, *298*, 869.

[7] a) J. B. Wittenberg, C. A. Appleby, B. A. Wittenberg, *J. Biol. Chem.* **1972**, *247*, 527; b) A. P. Kloek, J. Yang, F. S. Mathews, D. E. Goldberg, *J. Biol. Chem.* **1993**, *268*, 17669.

[8] a) J. Yang, A. P. Kloek, D. E. Goldberg, F. S. Mathews, *Proc. Natl. Acad. Sci. USA* **1995**, *92*, 4224; b) S. C. Huang, J. Huang, A. P. Kloek, D. E. Goldberg, J. M. Friedman, *J. Biol. Chem.* **1996**, *271*, 958.

[9] a) M. Momenteau, B. Loock, C. Tetreau, D. Lavalette, A. Croisy, C. Schaeffer, C. Huel, J.-M. Lhoste, *J. Chem. Soc. Perkin Trans. II* **1987**, 249; b) G. E. Wuenschell, C. Tetreau, D. Lavalette, C. A. Reed, *J. Am. Chem. Soc.* **1992**, *114*, 3346; c) C. K. Chang, Y. Liang, G. Aviles, *J. Am. Chem. Soc.* **1995**, *117*, 4191; d) A. Zingg, B. Felber, V. Gramlich, L. Fu, J. P. Collman, F. Diederich, *Helv. Chim. Acta.* **2002**, *85*, 333.

[10] a) M. Momenteau, C. A. Reed, *Chem. Rev.* **1994**, *94*, 659, and references therein; b) M. Momenteau, "Models of Hemoprotein Active Sites" in *Supramolecular Control of Structure and Reactivity* (Ed.: A. D. Hamilton), Wiley, New York, **1996**, pp. 155–223.

[11] a) J. P. Collman, R. R. Gagne, T. R. Halbert, J. C. Marchon, C. A. Reed, *J. Am. Chem. Soc.* **1973**, *95*, 7868; b) J. P. Collman, R. R. Gagne, C. A. Reed, T. R. Halbert, G. Lang, W. T. Robinson, *J. Am. Chem. Soc.* **1975**, *97*, 1427.

[12] a) T. Hashimoto, R. L. Dyer, M. L. Crossley, J. E. Baldwin, F. Basolo, *J. Am. Chem. Soc.* **1982**, *104*, 2101; b) M. R. Johnson, W. K. Seok, J. A. Ibers, *J. Am. Chem. Soc.* **1991**, *113*, 3998.

[13] T. G. Traylor, N. Koga, L. A. Deardurff, P. N. Swepston, J. A. Ibers, *J. Am. Chem. Soc.* **1984**, *106*, 5132.

[14] J. P. Collman, J. I. Brauman, T. J. Collins, B. Iverson, J. L. Sessler, *J. Am. Chem. Soc.* **1981**, *103*, 2450.

[15] a) E. Rose, B. Boitrel, M. Quelquejeu, A. Kossanyi, *Tetrahedron. Lett.* **1993**, *34*, 7267; b) E. Rose, A. Lecas, M. Quelquejeu, A. Kossanyi, B. Boitrel, *Coord. Chem. Rev.* **1998**, *178–180*, 1407; c) E. Rose, M. Quelquejeu, R. P. Pandian, A. Lecas-Nawrocka, A. Vilar, G. Ricart, J. P. Collman, Z. Wang, A. Straumanis, *Polyhedron*, **2000**, *19*, 581.

[16] a) A. Kossanyi, F. Tani, N. Nakamura, Y. Naruta, *Chem. Eur. J.* **2001**, *7*, 2862; b) M. Matsu-ura, F. Tani, Y. Naruta, *J. Am. Chem. Soc.* **2002**, *124*, 1941.

[17] We have already reported similar **TCP** complexes as models for cytochrome P450: a) F. Tani, S. Nakayama, M. Ichimura, N. Nakamura, Y. Naruta, *Chem. Lett.* **1999**, 729; b) M. Matsu-ura, F. Tani, S. Nakayama, N. Nakamura, Y. Naruta, *Angew. Chem.* **2000**, *112*, 2083; *Angew. Chem. Int. Ed.* **2000**, *39*, 1989; c) F. Tani, M. Matsu-ura, S. Nakayama, M. Ichimura, N. Nakamura, Y. Naruta, *J. Am. Chem. Soc.* **2001**, *123*, 1133; d) M. Matsu-ura, F. Tani, Y. Naruta, *Chem. Lett.* **2000**, 814; e) F. Tani, M. Matsu-ura, S. Nakayama, Y. Naruta, *Coord. Chem. Rev.* **2002**, *226*, 219.

[18] a) J. P. Collman, J. I. Brauman, B. L. Iverson, J. L. Sessler, R. M. Morris, G. H. Gibson, *J. Am. Chem. Soc.* **1983**, *105*, 3052; b) T. G. Traylor, S. Tsuchiya, D. Campbell, M. Mitchell, D. Stynes, N. Koga, *J. Am. Chem. Soc.* **1985**, *107*, 604.

[19] The titrations were evaluated according to $P(L) = [C_I]b\Delta\varepsilon P(L)/\Delta A - P_{1/2}(L)$, where $P(L)$ [Torr] represents the partial pressure of the added gas L, $P_{1/2}(L)$ [Torr] the partial pressure of L at half-saturation binding to the Fe^{II} porphyrin, ΔA the difference in optical absorbance of the solution of the Fe^{II} porphyrin at $P(L)$ and in the absence of L, $[C_I]$ the total metalloporphyrin concentration, b the path length of the cell, and $\Delta\varepsilon$ the difference in the molar extinction coefficients between the carbonylated or oxygenated and deoxygenated forms. The term $[C_I]b\Delta\varepsilon$ is a constant under the conditions of the measurement. From the plot of $P(L)$ versus $P(L)/\Delta A$, $P_{1/2}(L)$ was determined.

[20] a) T. G. Traylor, D. K. White, D. H. Campbell, A. P. Berzinis, *J. Am. Chem. Soc.* **1981**, *103*, 4932; b) E. Antonini, M. Brunori, in *Hemoglobin and Myoglobin and their Reactions with Ligands*, North Holland, Amsterdam, **1971**.

[21] a) Q. H. Gibson, *J. Biol. Chem.* **1970**, *245*, 3285; b) J. S. Olson, M. E. Andersen, Q. H. Gibson, *J. Biol. Chem.* **1971**, *246*, 5919; c) V. S. Sharma, M. R. Schmidt, H, M. Ranney, *J. Biol. Chem.* **1976**, *251*, 4267; d) R. C. Steinmeier, L. J. Parkhurst, *Biochemistry* **1975**, *14*, 1564.

[22] T. G. Traylor, M. J. Mitchell, S. Tsuchiya, D. H. Campbell, D. V. Stynes, N. Koga, *J. Am. Chem. Soc.* **1981**, *103*, 5234.

[23] T. G. Traylor, N. Koga, L. A. Deardurff, P. N. Swepston, J. A. Ibers, *J. Am. Chem. Soc.* **1984**, *106*, 5132.
[24] J. P. Collman, J. I. Brauman, K. M. Doxsee, J. L. Sessler, R. M. Morris, Q. H. Gibson, *Inorg. Chem.* **1983**, *22*, 1427.
[25] M. Momenteau, B. Loock, D. Lavalette, C. Tetreau, J. Mispelter, *J. Chem. Soc. Chem. Commun.* **1983**, 962.
[26] High selectivity toward O_2 binding has also been reported in bis-handle porphyrin.[15]
[27] M. Y. R. Wang, B. M. Hoffman, S. J. Shire, F. R. N. Gurd, *J. Am. Chem. Soc.* **1979**, *101*, 7394.
[28] a) K. Imai, T. Yonetani, *J. Biol. Chem.* **1975**, *250*, 7093; b) K. Imai, I. Tyuma, *Biochem. Biophys. Res. Commun.* **1973**, *51*, 52.
[29] a) J. P. Collman, J. I. Brauman, K. M. Doxsee, T. R. Halbert, K. S. Suslick, *Proc. Natl. Acad. Sci. USA* **1978**, *75*, 564; b) J. P. Collman, J. I. Brauman, K. M. Doxsee, T. R. Halbert, S. E. Hayers, K. S. Suslick, *J. Am. Chem. Soc.* **1978**, *100*, 2761.
[30] J. E. Linard, P. E. Ellis, Jr., J. R. Budge, R. D. Jones, F. Basolo, *J. Am. Chem. Soc.* **1980**, *102*, 1896.
[31] K. S. Suslick, M. M. Fox, *J. Am. Chem. Soc.* **1983**, *105*, 3507.
[32] The thermodynamic parameters for the oxygenation of **TCP-IM** and **TCP-PY** were obtained by determining $P_{1/2}(O_2)$ in the temperature range of 25 to $-40\,^{\circ}$C. ΔH and ΔS were determined from least-squares fits to the van't Hoff equation.
[33] a) P. Maillard, C. Schaeffer, C. Tetreau, D. Lavalette, J-M. Lhoste, M. Momenteau, *J. Chem. Soc. Perkin. Trans. II* **1989**, 1437; b) D. Lavalette, C. Tetreau, J. Mispelter, M. Momenteau, J-M. Lhoste, *Eur. J. Biochem.* **1984**, *145*, 555; c) C. Tetreau, B. Boitrel, E. Rose, D. Lavalette, *J. Chem. Soc. Chem. Commun.* **1989**, 1805.
[34] a) J. Geibel, J. Cannon, D. Campbell, T. G. Traylor, *J. Am. Chem. Soc.* **1978**, *100*, 3575; b) T. G. Traylor, *Acc. Chem. Res.* **1981**, *14*, 102.
[35] Because the cavities of **TCP**s are relatively small and the short arm supporting the axial ligand is not flexible enough, it can be speculated that the axial ligand may not adopt an optimal geometry. However, it has been reported that the RR spectra of the imidazole-appended hemes showed an insensitivity of ν(Fe–O_2) to a constraint introduced by the length or the nature of the chain bearing the imidazole residue. N.-T. Yu, H. M. Thompson, C. K. Chang, *Biophys. J.* **1987**, *51*, 283.
[36] a) J. Ramsden, T. G. Spiro, *Biochemistry*, **1989**, *28*, 3125; b) W. H. Fuchsman, C. A. Appleby, *Biochemistry* **1979**, *18*, 1309; c) T. Perkins, J. D. Satterlee, J. H. Richards, *J. Am. Chem. Soc.* **1983**, *105*, 1350.
[37] a) M. Tsubaki, R. B. Srivastava, N.-T. Yu, *Biochemistry* **1982**, *21*, 1132; b) R. B. Moon, J. H. Richards, *Biochemistry* **1974**, *13*, 3437.
[38] a) E. A. Kerr, H. C. Mackin, N.-T. Yu, *Biochemistry* **1983**, *22*, 4373; b) E. A. Kerr, Ph.D. Dissertation, Georgia Institute of Technology, Atlanta, GA, 1984; c) C. G. Kalodimos, I. P. Gerothanassis, R. Pierattelli, B. Ancian, *Inorg. Chem.* **1999**, *38*, 4283.
[39] J. P. Collman, J. I. Brauman, T. J. Collins, B. L. Iverson, G. Lang, R. B. Pettman, J. L. Sessler, M. A. Walters, *J. Am. Chem. Soc.* **1983**, *105*, 3038.
[40] A. Desbois, M. Momenteau, M. Lutz, *Inorg. Chem.* **1989**, *28*, 825.
[41] G. B. Ray, X-Y. Li, J. A. Ibers, J. L. Sessler, T. G. Spiro, *J. Am. Chem. Soc.* **1994**, *116*, 162.
[42] Similar significant shieldings of the ^{13}C resonance were reported in bis-handle porphyrins ($\delta = 199.4$ and 202.7 ppm, B. Boitrel, A. Lecas-Nawrocka, E. Rose, *Tetrahedron Lett.* **1991**, *32*, 2129) and C_2-Cap porphyrin.[38c] These strong shieldings were ascribed to the π-electron clouds of the appended benzene ring.
[43] T. G. Spiro in *Biological Applications of Raman Spectroscopy*, *Vol. 3*, Wiley, New York, **1988**.
[44] The ν_4 bands of the CO adducts were observed at 1364 (**TCP-IM**) and 1363 cm^{-1} (**TCP-PY**).
[45] We could not observe the ν(O–O) mode of oxy-**TCP**s in IR spectra because it would overlap with strong IR bands of the **TCP** ligand in 1000 – 1200 cm^{-1} region.
[46] a) A. Bruha, J. R. Kincaid, *J. Am. Chem. Soc.* **1988**, *110*, 6006; b) L. M. Proniewicz, J. R. Kincaid, *Coord. Chem. Rev.* **1997**, *161*, 881.
[47] H. Brunner, *Naturwissenschaften* **1974**, *61*, 129.
[48] a) M. Tsubaki, N.-T. Yu, *Proc. Natl. Acad. Sci. USA* **1981**, *78*, 3581; b) L. M. Proniewicz, J. R. Kincaid, *J. Am. Chem. Soc.* **1990**, *112*, 675.
[49] T. K. Das, M. Couture, Y. Ouellet, M. Guertin, D. L. Rousseau, *Proc. Natl. Acad. Sci. USA* **2001**, *98*, 479.
[50] W. D. Wagner, I. R. Paeng, K. Nakamoto, *J. Am. Chem. Soc.* **1988**, *110*, 5556.
[51] S. Nakayama, F. Tani, M. Matsu-ura, Y. Naruta, *Chem. Lett.* **2002**, 496.
[52] a) E. A. Kerr, N.-T. Yu, D. E. Bartnicki, H. Mizukami, *J. Biol. Chem.* **1985**, *260*, 8360; b) S. Hirota, T.Ogura, E. H. Appelman, K. Shinzawa-Itoh, S. Yoshikawa, T. Kitagawa, *J. Am. Chem. Soc.* **1994**, *116*, 10564.
[53] a) K. Nagai, T. Kitagawa, H. Morinoto, *J. Mol. Biol.* **1980**, *136*, 271; b) M. A. Walters, T. G. Spiro, *Biochemistry* **1982**, *21*, 6989.
[54] M. A. Walters, T. G. Spiro, K. S. Suslick, J. P. Collman, *J. Am. Chem. Soc.* **1980**, *102*, 6857.
[55] W. A. Oertling, R. T. Kean, T. Weaver, C. T. Babcock, *Inorg. Chem.* **1990**, *29*, 2633.
[56] Control experiments were performed for the CO adducts, but we could not observe any ν(Fe–CO) frequency shifts on temperature change.
[57] J. Odo, H. Imai, E. Kyuno, K. Nakamoto, *J. Am. Chem. Soc.* **1988**, *110*, 742.
[58] We have also reported direct evidence for hydrogen bonding between the adjacent hydroxyl groups and bound O_2 in thiolate-coordinated oxy-**TCP**s: the ν(O–O) bands in RR spectra shifted by 2 cm^{-1} in the H/D exchange experiments.[15b,c]

Received: August 12, 2002 [F4338]

  0947-6539/03/0904-0870 $ 20.00+.50/0